Properties of spinel-type Ti-Li-M composite oxides (M = Li, Na, Cu, and Ag) predicted by density functional theory: Supplementary Information

Kohei Tada[#], Mitsunori Kitta, Shingo Tanaka

Table S1 Direct coordinates of 8a sites in the 1×1×3 supercell model.

Site index	x	y	z
1	0.0	0.0	0.0
2	0.0	0.5	0.166666667
3	0.5	0.5	0.0
4	0.5	0.0	0.166666667
5	0.75	0.25	0.25
6	0.25	0.25	0.083333333
7	0.25	0.75	0.25
8	0.75	0.75	0.083333333
9	0.0	0.0	0.333333333
10	0.0	0.5	0.5
11	0.5	0.5	0.333333333
12	0.5	0.0	0.5
13	0.75	0.25	0.583333333
14	0.25	0.25	0.416666667
15	0.25	0.75	0.583333333
16	0.75	0.75	0.416666667
17	0.0	0.0	0.666666667
18	0.0	0.5	0.833333333
19	0.5	0.5	0.666666667
20	0.5	0.0	0.833333333
21	0.75	0.25	0.916666667
22	0.25	0.25	0.75
23	0.25	0.75	0.916666667
24	0.75	0.75	0.75

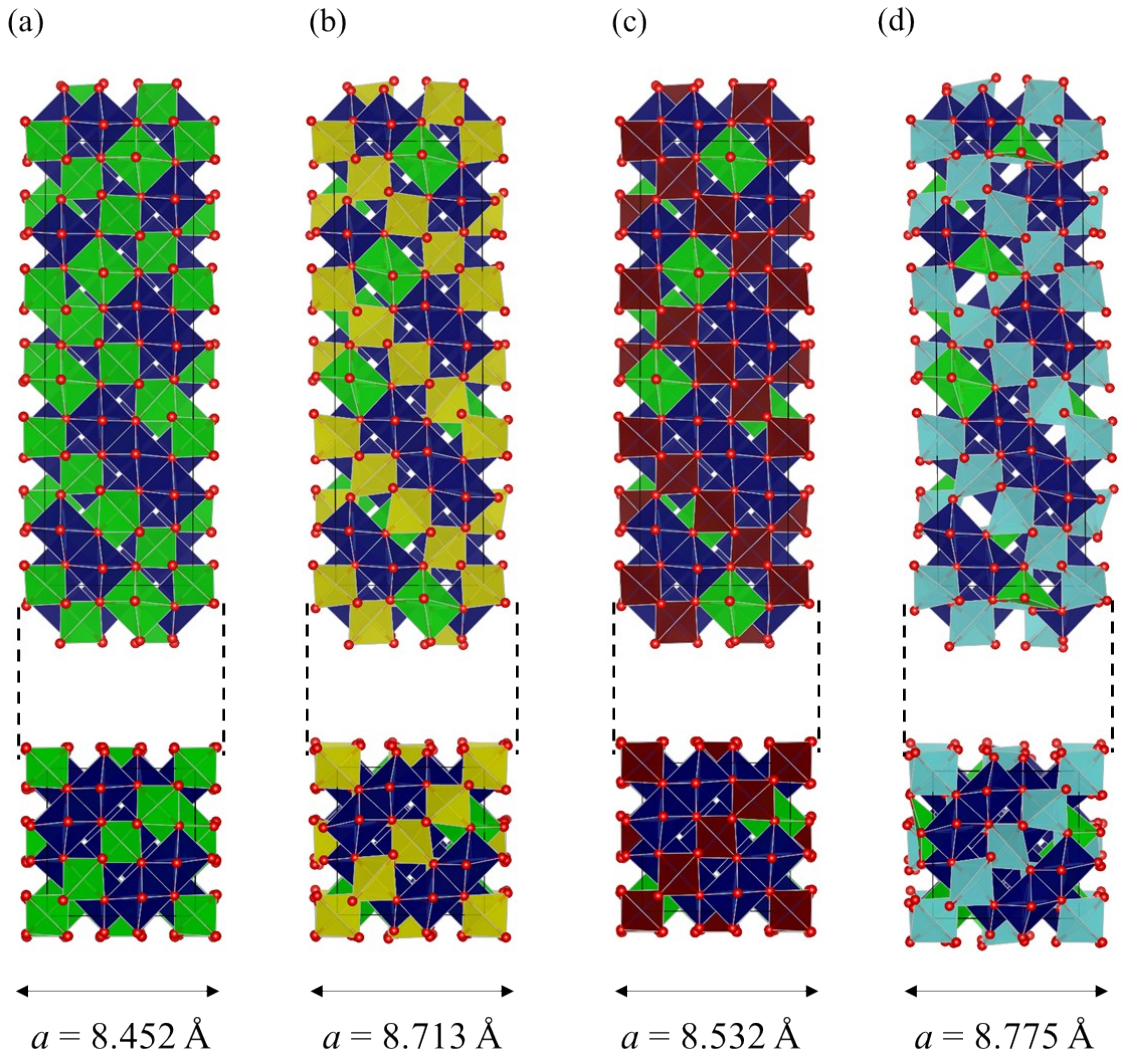

Fig. S1. Optimised structures of LTO (a), NTO (b), CTO (c), and ATO (d) supercell models by PBE+*U* (*U* = 3.0 eV). Green, dark blue, yellow, brown, light blue, and red colours indicate Li, Ti, Na, Cu, Ag, and O, respectively. Upper and lower panels show side and top views, respectively.

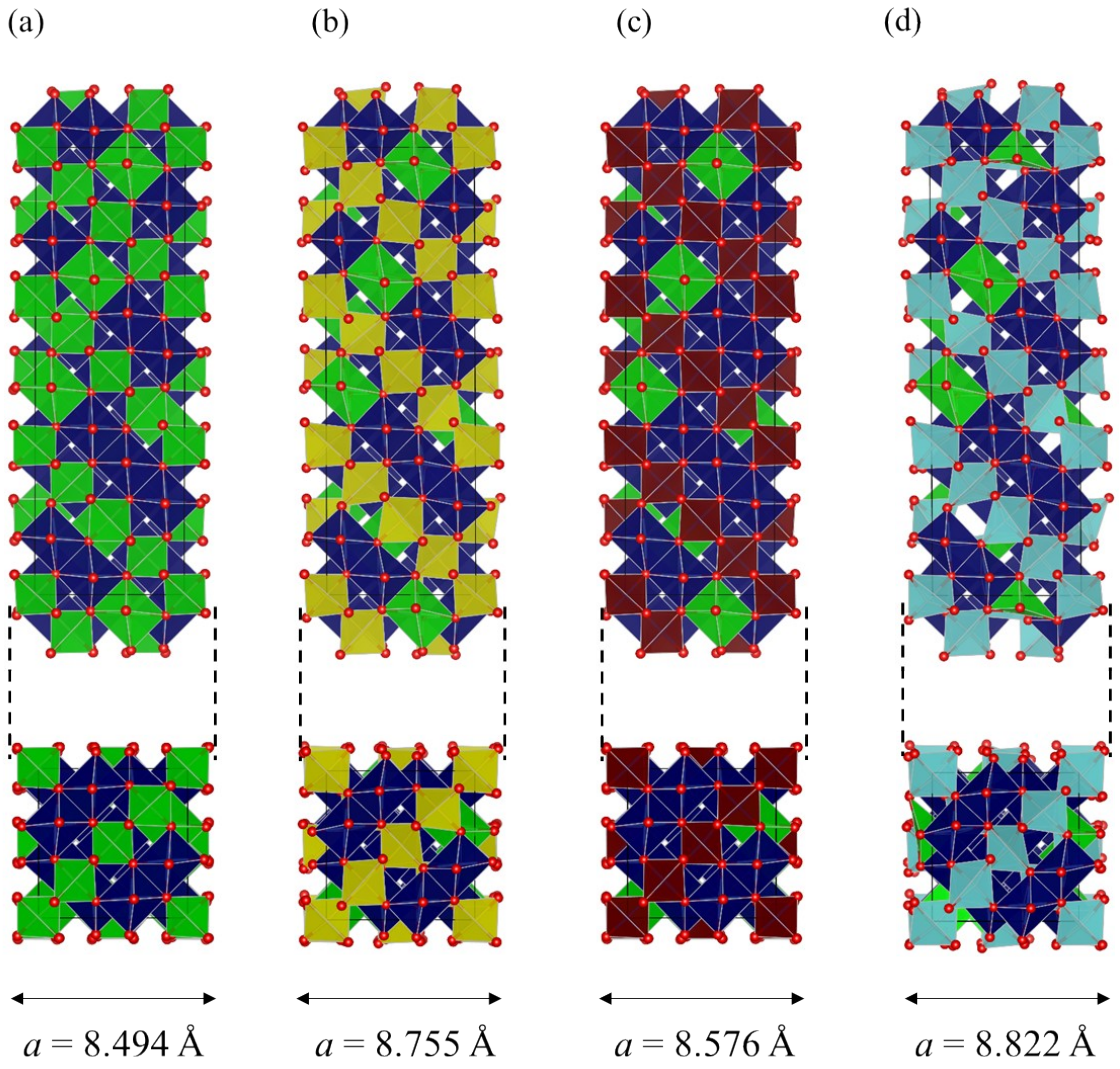

Fig. S2. Optimised structures of LTO (a), NTO (b), CTO (c), and ATO (d) supercell models by PBE+*U* (*U* = 5.0 eV). Green, dark blue, yellow, brown, light blue, and red colours indicate Li, Ti, Na, Cu, Ag, and O, respectively. Upper and lower panels show side and top views, respectively.

Table S2. Lattice parameters and cell volumes of optimised LTO, NTO, CTO, and ATO supercell models by GGA-PBE.

	LTO	NTO	CTO	ATO
a [Å]	8.39615	8.71225	8.46933	8.74662
b [Å]	8.40822	8.68967	8.48573	8.79603
c/3 [Å]	8.39855	8.75372	8.47574	8.89934
alpha [°]	89.9156	90.3443	89.9608	90.6199
beta [°]	90.0748	89.7019	90.0239	89.7046
gamma [°]	90.0016	90.0170	89.9958	90.0547
V/3 [Å^3]	592.91	662.69	609.14	684.63

Table S3. Lattice parameters and cell volumes of optimised LTO, NTO, CTO, and ATO supercell models by PBE+*U* (*U* = 3.0 eV).

	LTO	NTO	CTO	ATO
a [Å]	8.45224	8.71279	8.53208	8.77479
b [Å]	8.46574	8.76090	8.54160	8.86615
c/3 [Å]	8.44920	8.77771	8.53184	8.93323
alpha [°]	89.8734	90.2339	89.9056	90.4406
beta [°]	90.1054	89.8210	90.0649	89.7687
gamma [°]	90.0034	89.9970	89.9960	89.9820
V/3 [Å^3]	604.58	670.01	621.78	694.97

Table S4. Lattice parameters and cell volumes of optimised LTO, NTO, CTO, and ATO supercell models by PBE+*U* (*U* = 5.0 eV).

	LTO	NTO	CTO	ATO
a [Å]	8.49373	8.75483	8.57561	8.82201
b [Å]	8.50095	8.79488	8.57887	8.90129
c/3 [Å]	8.48586	8.80735	8.57249	8.96390
alpha [°]	89.8479	90.1943	89.8631	90.3646
beta [°]	90.1294	89.8520	90.0963	89.8247
gamma [°]	90.0042	90.0009	89.9967	89.9561
V/3 [Å^3]	612.72	678.14	630.67	703.89

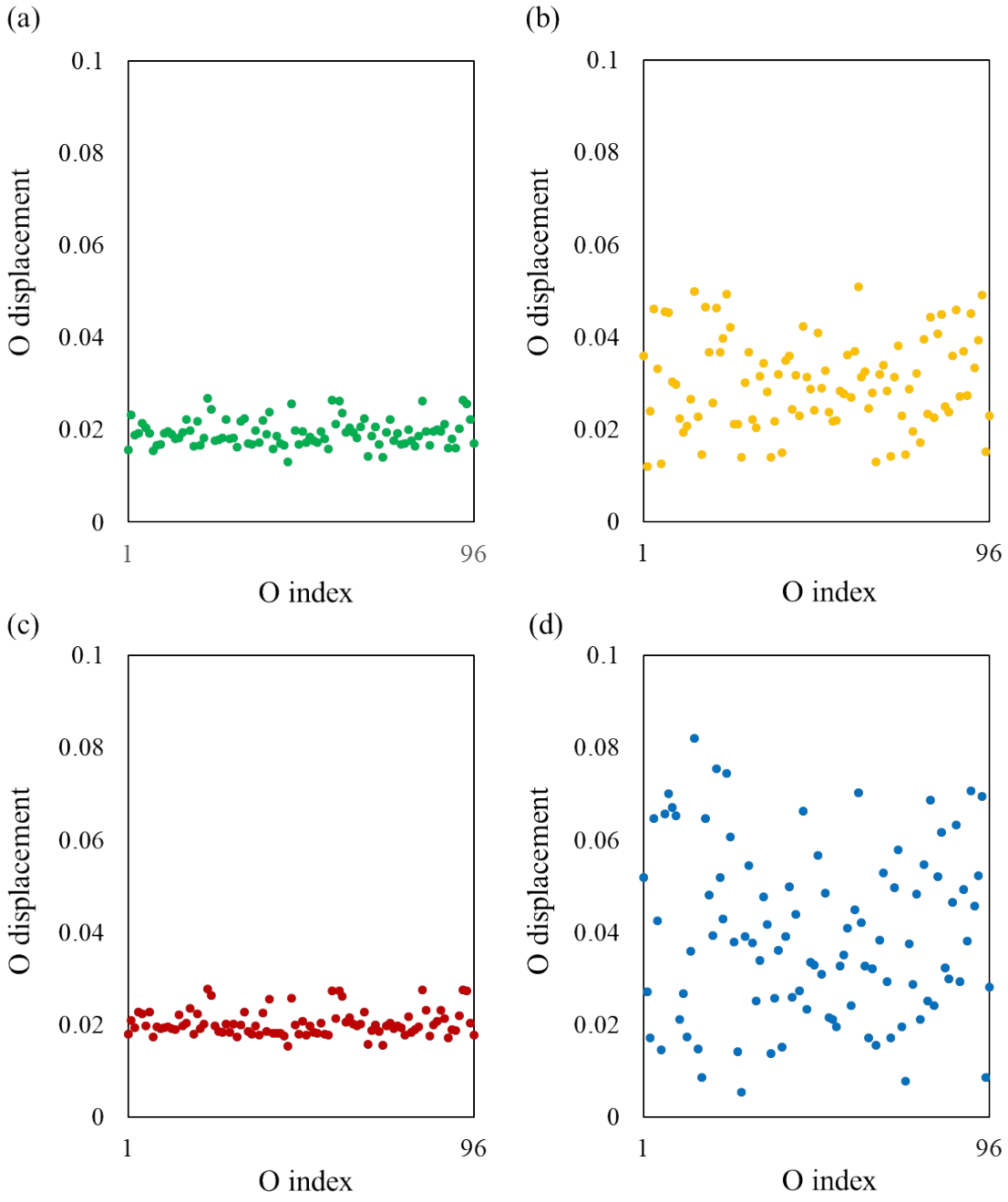

Fig. S3. O displacements of LTO, NTO, CTO, and ATO by PBE+*U* (*U* = 3 eV)

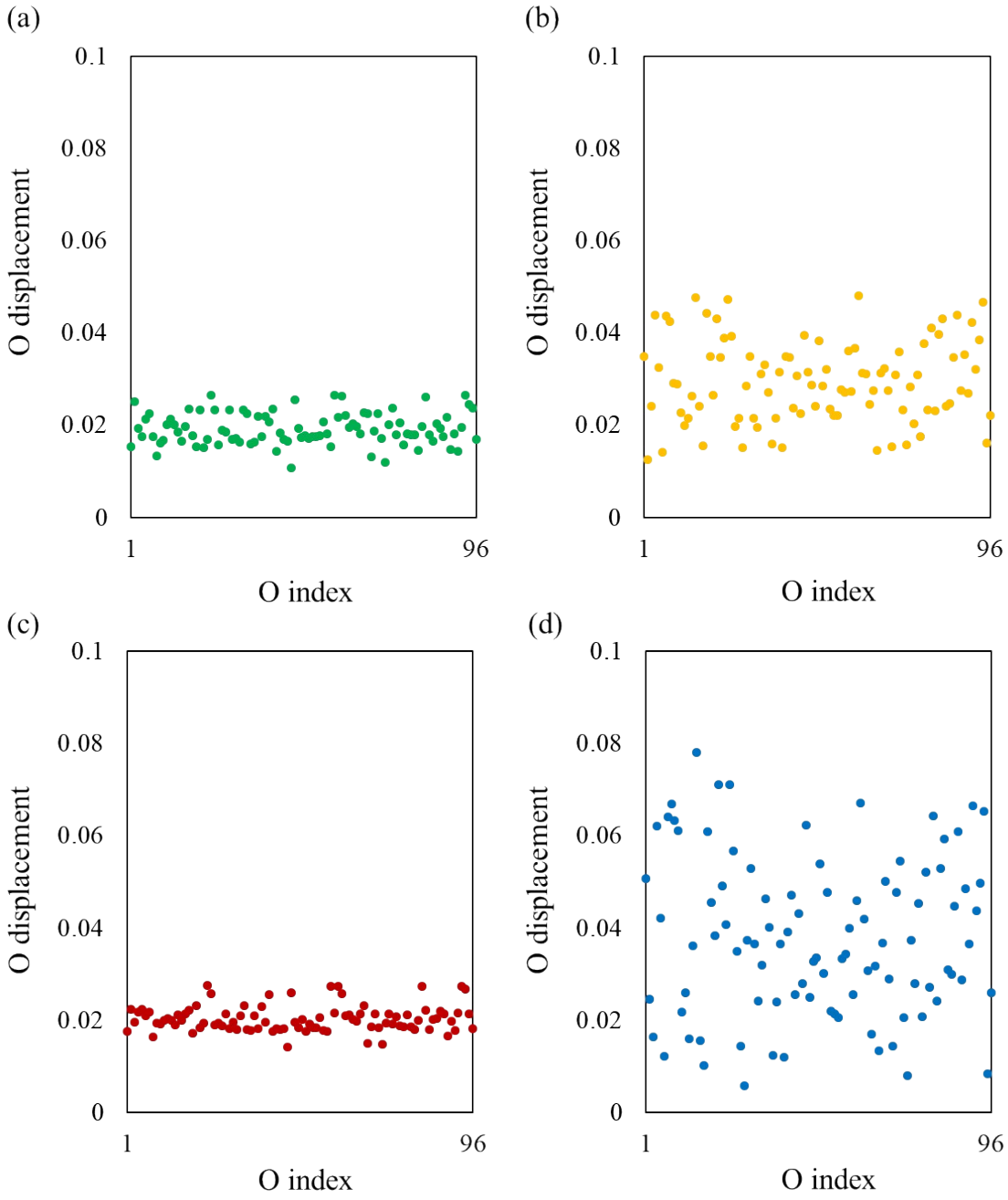

Fig. S4. O displacements of LTO, NTO, CTO, and ATO by PBE+*U* (*U* = 5 eV)

Table S5. Maximum, minimum, medium, average, and standard derivation values of O displacements in LTO, NTO, CTO, and ATO estimated by GGA-PBE results.

	LTO	NTO	CTO	ATO
Maximum	0.02794	0.05882	0.02867	0.08702
Minimum	0.01578	0.01058	0.01652	0.00875
Median	0.01910	0.02999	0.01955	0.03929
Average	0.01977	0.03205	0.02052	0.04275
Standard deviation	0.00285	0.01148	0.00313	0.02049

Table S6. Maximum, minimum, medium, average, and standard derivation values of O displacements of LTO, NTO, CTO, and ATO estimated by PBE+*U* (*U* = 3 eV) results.

	LTO	NTO	CTO	ATO
Maximum	0.02687	0.05083	0.02774	0.08202
Minimum	0.01313	0.01203	0.01536	0.00530
Median	0.01901	0.02936	0.01971	0.03781
Average	0.01935	0.03015	0.02030	0.03922
Standard deviation	0.00293	0.00988	0.00281	0.01827

Table S7. Maximum, minimum, medium, average, and standard derivation values of O displacements of LTO, NTO, CTO, and ATO estimated by PBE+*U* (*U* = 5 eV) results.

	LTO	NTO	CTO	ATO
Maximum	0.02651	0.04808	0.02747	0.07800
Minimum	0.01068	0.01256	0.01423	0.00571
Median	0.01842	0.02853	0.01978	0.03651
Average	0.01912	0.02943	0.02028	0.03784
Standard deviation	0.00343	0.00887	0.00282	0.01722

Table S8. Estimated bandgaps of LTO, NTO, CTO, and ATO by hybrid-DFT (HSE06) and DFT+*U* (*U* = 0.0, 3.0, and 5.0 eV).

Compound	Bandgap (HSE06) [eV]	Bandgap (*U* = 0.0 eV) [eV]	Bandgap (*U* = 3.0 eV) [eV]	Bandgap (*U* = 5.0 eV) [eV]
LTO	4.25	2.68	2.85	3.03
NTO	4.37	2.79	2.80	2.96
CTO	1.63	0.60	0.64	0.72
ATO	2.85	1.49	1.53	1.69

Table S9. Maximum, minimum, median, and average values of E_{Odef} in eV of LTO, NTO, CTO, and ATO.

	LTO	NTO	CTO	ATO
Maximum	5.55	5.31	5.26	3.64
Minimum	4.28	3.86	4.06	2.40
Median	5.04	4.56	4.475	2.99
Average	5.04	4.59	4.47	2.99

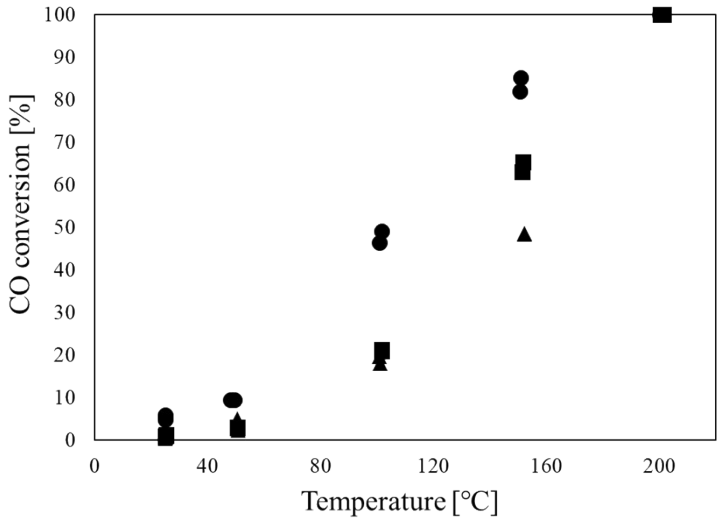

Fig. S5. CO oxidation activities of spinel-type Ag-titanates. ●: 1st, ■: 2nd, and ▲: 3rd cycles.

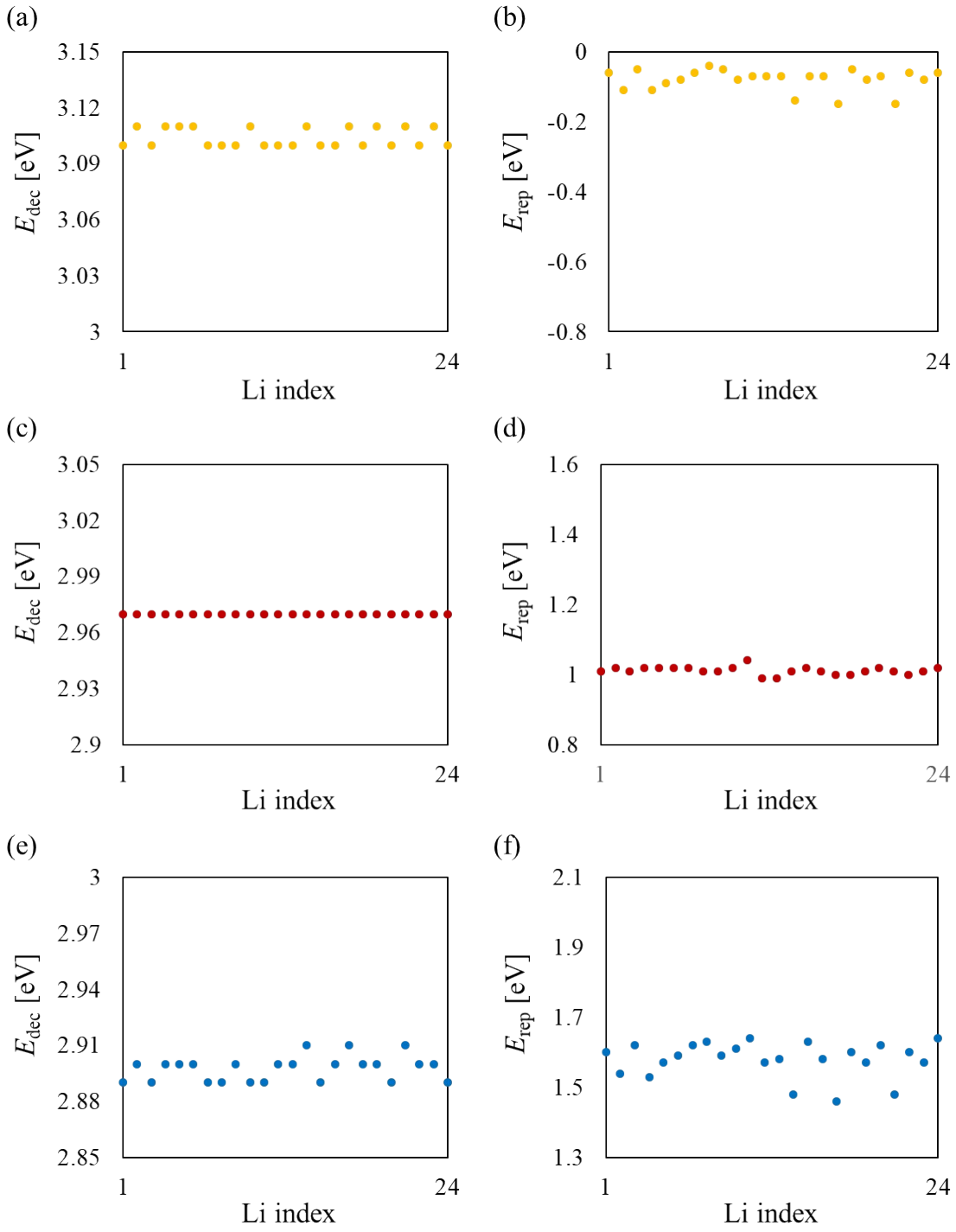

Fig. S6. (a) E_{dec} of the Na-LTO, (b) E_{rep} of the Na-LTO, (c) E_{dec} of the Cu-LTO, (d) E_{rep} of the Cu-LTO, (e) E_{dec} of the Ag-LTO, (f) E_{rep} of the Ag-LTO. The specific values are shown in Table S10.

Table S10. Decomposition energies (E_{dec}) and dope reaction energies (E_{rep}) of X-LTO (X = Na, Cu, and Ag) systems.

Site index	X = Na		X = Cu		X = Ag	
	E_{dec} [eV]	E_{rep} [eV]	E_{dec} [eV]	E_{rep} [eV]	E_{dec} [eV]	E_{rep} [eV]
1	3.10	-0.06	2.97	1.01	2.89	1.60
2	3.11	-0.11	2.97	1.02	2.90	1.54
3	3.10	-0.05	2.97	1.01	2.89	1.62
4	3.11	-0.11	2.97	1.02	2.90	1.53
5	3.11	-0.09	2.97	1.02	2.90	1.57
6	3.11	-0.08	2.97	1.02	2.90	1.59
7	3.10	-0.06	2.97	1.02	2.89	1.62
8	3.10	-0.04	2.97	1.01	2.89	1.63
9	3.10	-0.05	2.97	1.01	2.90	1.59
10	3.11	-0.08	2.97	1.02	2.89	1.61
11	3.10	-0.07	2.97	1.04	2.89	1.64
12	3.10	-0.07	2.97	0.99	2.90	1.57
13	3.10	-0.07	2.97	0.99	2.90	1.58
14	3.11	-0.14	2.97	1.01	2.91	1.48
15	3.10	-0.07	2.97	1.02	2.89	1.63
16	3.10	-0.07	2.97	1.01	2.90	1.58
17	3.11	-0.15	2.97	1.00	2.91	1.46
18	3.10	-0.05	2.97	1.00	2.90	1.60
19	3.11	-0.08	2.97	1.01	2.90	1.57
20	3.10	-0.07	2.97	1.02	2.89	1.62
21	3.11	-0.15	2.97	1.01	2.91	1.48
22	3.10	-0.06	2.97	1.00	2.90	1.60
23	3.11	-0.08	2.97	1.01	2.90	1.57
24	3.10	-0.06	2.97	1.02	2.89	1.64

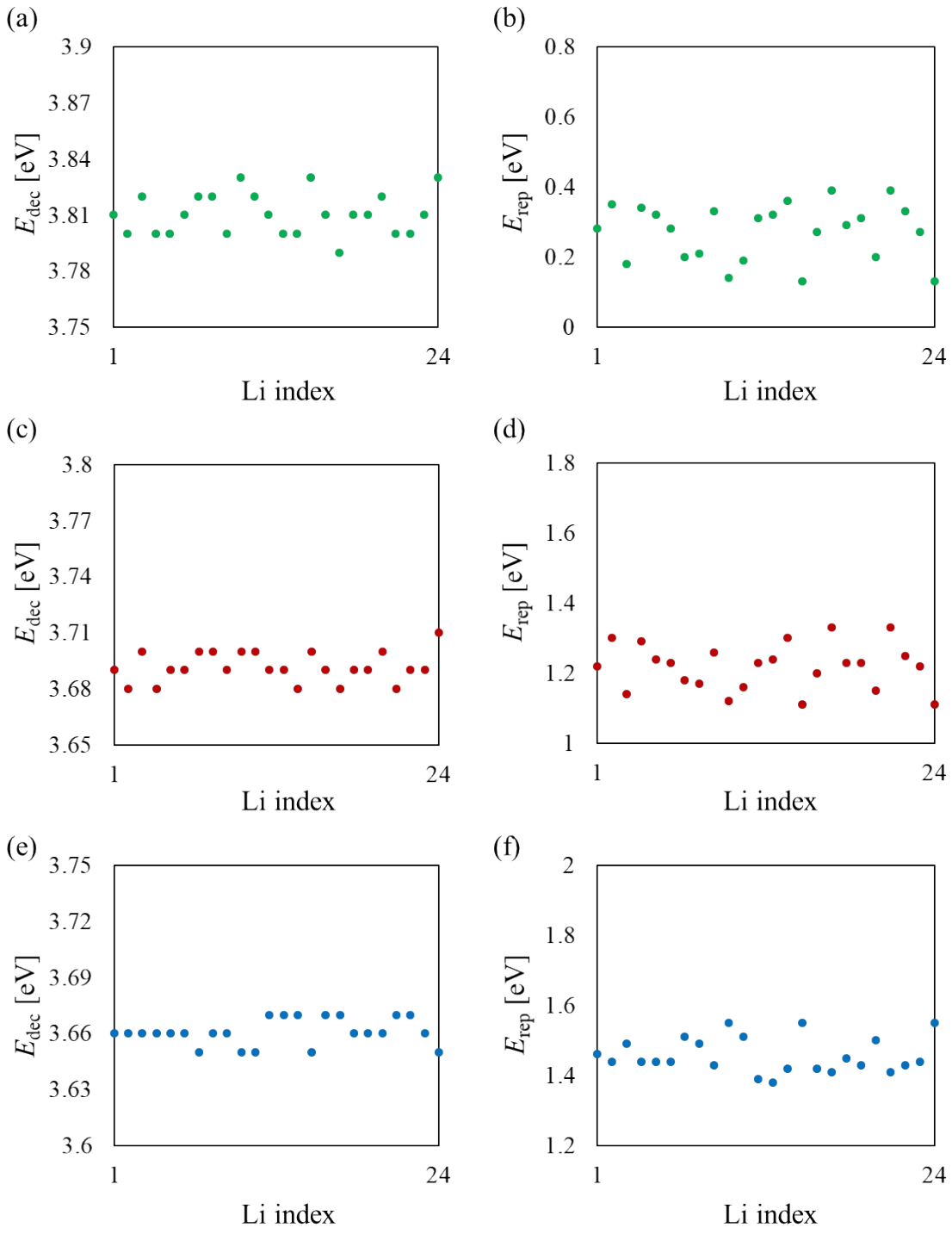

Fig. S7. (a) E_{dec} of the Li-NTO, (b) E_{rep} of the Li-NTO, (c) E_{dec} of the Cu-NTO, (d) E_{rep} of the Cu-NTO, (e) E_{dec} of the Ag-NTO, (f) E_{rep} of the Ag-NTO. The specific values are shown in Table S11.

Table S11. Decomposition energies (E_{dec}) and dope reaction energies (E_{rep}) of X-NTO (X = Li, Cu, and Ag) systems.

Site index	X = Li		X = Cu		X = Ag	
	E_{dec} [eV]	E_{rep} [eV]	E_{dec} [eV]	E_{rep} [eV]	E_{dec} [eV]	E_{rep} [eV]
1	3.81	0.28	3.69	1.22	3.66	1.46
2	3.80	0.35	3.68	1.30	3.66	1.44
3	3.82	0.18	3.70	1.14	3.66	1.49
4	3.80	0.34	3.68	1.29	3.66	1.44
5	3.80	0.32	3.69	1.24	3.66	1.44
6	3.81	0.28	3.69	1.23	3.66	1.44
7	3.82	0.20	3.70	1.18	3.65	1.51
8	3.82	0.21	3.70	1.17	3.66	1.49
9	3.80	0.33	3.69	1.26	3.66	1.43
10	3.83	0.14	3.70	1.12	3.65	1.55
11	3.82	0.19	3.70	1.16	3.65	1.51
12	3.81	0.31	3.69	1.23	3.67	1.39
13	3.80	0.32	3.69	1.24	3.67	1.38
14	3.80	0.36	3.68	1.30	3.67	1.42
15	3.83	0.13	3.70	1.11	3.65	1.55
16	3.81	0.27	3.69	1.20	3.67	1.42
17	3.79	0.39	3.68	1.33	3.67	1.41
18	3.81	0.29	3.69	1.23	3.66	1.45
19	3.81	0.31	3.69	1.23	3.66	1.43
20	3.82	0.20	3.70	1.15	3.66	1.50
21	3.80	0.39	3.68	1.33	3.67	1.41
22	3.80	0.33	3.69	1.25	3.67	1.43
23	3.81	0.27	3.69	1.22	3.66	1.44
24	3.83	0.13	3.71	1.11	3.65	1.55

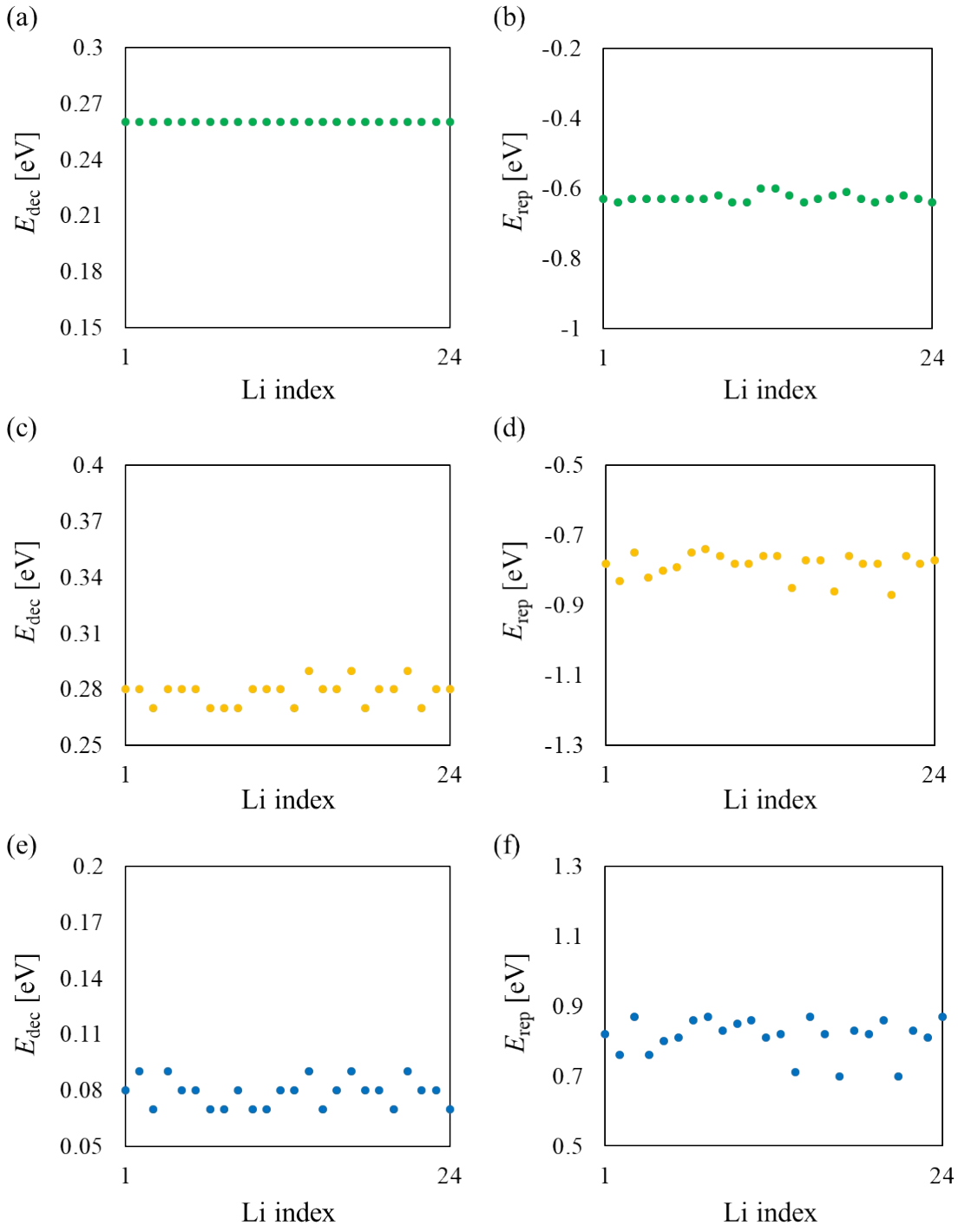

Fig. S8. (a) E_{dec} of the Li-CTO, (b) E_{rep} of the Li-CTO, (c) E_{dec} of the Na-CTO, (d) E_{rep} of the Na-CTO, (e) E_{dec} of the Ag-CTO, (f) E_{rep} of the Ag-CTO. The specific values are shown in Table S12.

Table S12. Decomposition energies (E_{dec}) and dope reaction energies (E_{rep}) of X-CTO (X = Li, Na, and Ag) systems.

Site index	X = Li		X = Na		X = Ag	
	E_{dec} [eV]	E_{rep} [eV]	E_{dec} [eV]	E_{rep} [eV]	E_{dec} [eV]	E_{rep} [eV]
1	0.26	-0.63	0.28	-0.78	0.08	0.82
2	0.26	-0.64	0.28	-0.83	0.09	0.76
3	0.26	-0.63	0.27	-0.75	0.07	0.87
4	0.26	-0.63	0.28	-0.82	0.09	0.76
5	0.26	-0.63	0.28	-0.80	0.08	0.80
6	0.26	-0.63	0.28	-0.79	0.08	0.81
7	0.26	-0.63	0.27	-0.75	0.07	0.86
8	0.26	-0.63	0.27	-0.74	0.07	0.87
9	0.26	-0.62	0.27	-0.76	0.08	0.83
10	0.26	-0.64	0.28	-0.78	0.07	0.85
11	0.26	-0.64	0.28	-0.78	0.07	0.86
12	0.26	-0.60	0.28	-0.76	0.08	0.81
13	0.26	-0.60	0.27	-0.76	0.08	0.82
14	0.26	-0.62	0.29	-0.85	0.09	0.71
15	0.26	-0.64	0.28	-0.77	0.07	0.87
16	0.26	-0.63	0.28	-0.77	0.08	0.82
17	0.26	-0.62	0.29	-0.86	0.09	0.70
18	0.26	-0.61	0.27	-0.76	0.08	0.83
19	0.26	-0.63	0.28	-0.78	0.08	0.82
20	0.26	-0.64	0.28	-0.78	0.07	0.86
21	0.26	-0.63	0.29	-0.87	0.09	0.70
22	0.26	-0.62	0.27	-0.76	0.08	0.83
23	0.26	-0.63	0.28	-0.78	0.08	0.81
24	0.26	-0.64	0.28	-0.77	0.07	0.87

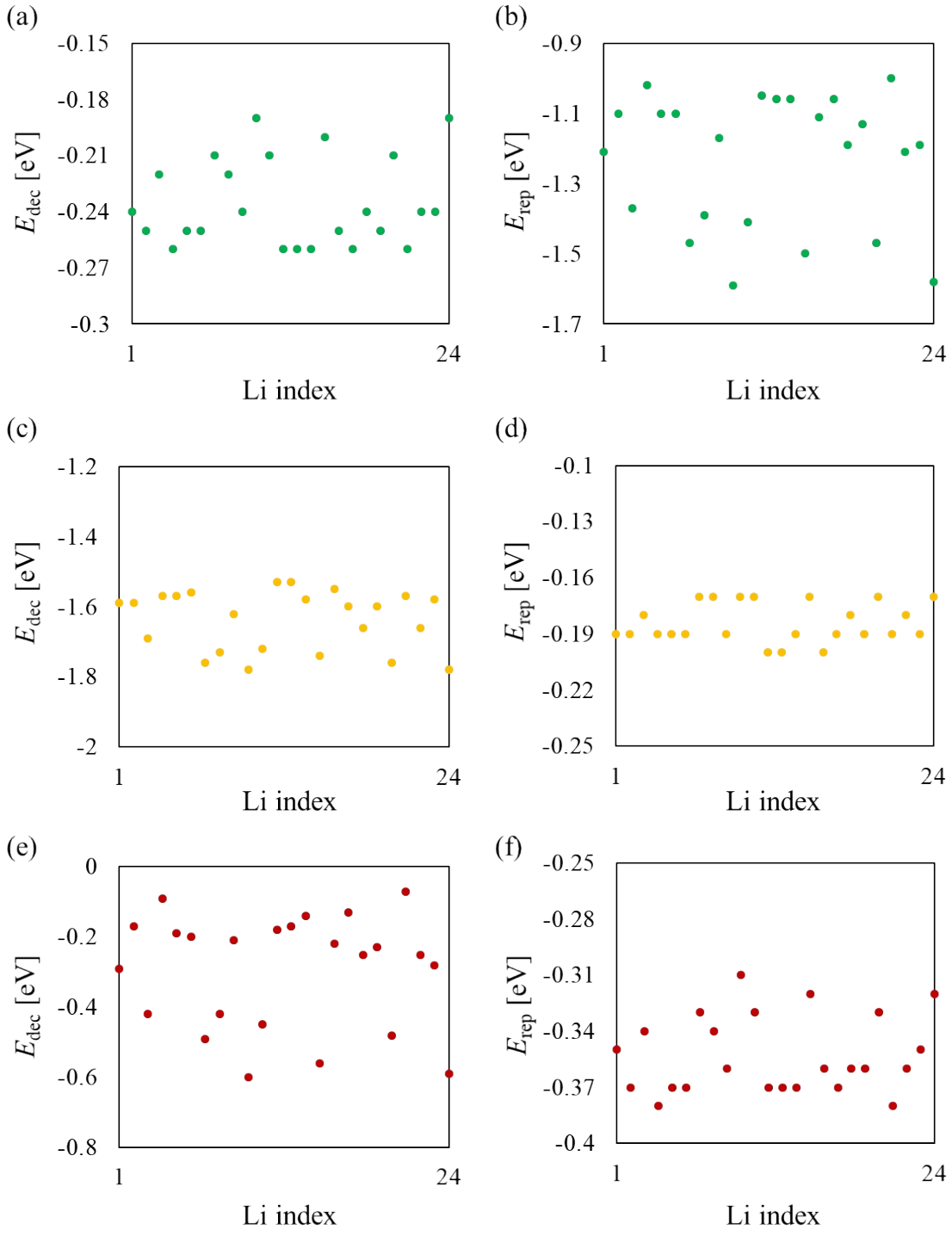

Fig. S9. (a) E_{dec} of the Li-ATO, (b) E_{rep} of the Li-ATO, (c) E_{dec} of the Na-ATO, (d) E_{rep} of the Na-ATO, (e) E_{dec} of the Cu-ATO, (f) E_{rep} of the Cu-ATO. The specific values are shown in Table S13.

Table S13. Decomposition energies (E_{dec}) and dope reaction energies (E_{rep}) of X-ATO (X = Li, Na, and Cu) systems.

Site index	X = Li		X = Na		X = Cu	
	E_{dec} [eV]	E_{rep} [eV]	E_{dec} [eV]	E_{rep} [eV]	E_{dec} [eV]	E_{rep} [eV]
1	-0.24	-1.21	-0.19	-1.59	-0.35	-0.29
2	-0.25	-1.10	-0.19	-1.59	-0.37	-0.17
3	-0.22	-1.37	-0.18	-1.69	-0.34	-0.42
4	-0.26	-1.02	-0.19	-1.57	-0.38	-0.09
5	-0.25	-1.10	-0.19	-1.57	-0.37	-0.19
6	-0.25	-1.10	-0.19	-1.56	-0.37	-0.2
7	-0.21	-1.47	-0.17	-1.76	-0.33	-0.49
8	-0.22	-1.39	-0.17	-1.73	-0.34	-0.42
9	-0.24	-1.17	-0.19	-1.62	-0.36	-0.21
10	-0.19	-1.59	-0.17	-1.78	-0.31	-0.60
11	-0.21	-1.41	-0.17	-1.72	-0.33	-0.45
12	-0.26	-1.05	-0.20	-1.53	-0.37	-0.18
13	-0.26	-1.06	-0.20	-1.53	-0.37	-0.17
14	-0.26	-1.06	-0.19	-1.58	-0.37	-0.14
15	-0.20	-1.50	-0.17	-1.74	-0.32	-0.56
16	-0.25	-1.11	-0.20	-1.55	-0.36	-0.22
17	-0.26	-1.06	-0.19	-1.60	-0.37	-0.13
18	-0.24	-1.19	-0.18	-1.66	-0.36	-0.25
19	-0.25	-1.13	-0.19	-1.60	-0.36	-0.23
20	-0.21	-1.47	-0.17	-1.76	-0.33	-0.48
21	-0.26	-1.00	-0.19	-1.57	-0.38	-0.07
22	-0.24	-1.21	-0.18	-1.66	-0.36	-0.25
23	-0.24	-1.19	-0.19	-1.58	-0.35	-0.28
24	-0.19	-1.58	-0.17	-1.78	-0.32	-0.59

Table S14 Band gaps (eV) of the X-LTO system estimated by hybrid-DFT calculation (HSE06).

Replaced site	X = Na	X = Cu	X = Ag
1	4.27	1.93	3.05
2	4.28	1.92	3.10
3	4.28	1.97	3.06
4	4.28	1.88	3.07
5	4.27	1.95	3.09
6	4.28	1.91	3.05
7	4.28	2.00	3.12
8	4.28	1.99	3.09
9	4.27	1.97	3.08
10	4.29	1.90	3.01
11	4.28	1.98	3.13
12	4.28	1.94	3.05
13	4.28	1.91	3.04
14	4.26	1.90	3.07
15	4.29	1.91	3.01
16	4.27	1.91	3.05
17	4.27	1.88	3.05
18	4.28	1.95	3.06
19	4.25	1.91	3.05
20	4.25	1.96	3.08
21	4.28	1.84	3.03
22	4.28	1.95	3.06
23	4.28	1.92	3.05
24	4.27	1.97	3.07

Table S15 Band gaps (eV) of the X-NTO system estimated by hybrid-DFT calculation (HSE06).

Replaced site	X = Li	X = Cu	X = Ag
1	4.39	2.03	3.25
2	4.38	2.05	3.38
3	4.41	2.05	3.26
4	4.39	1.98	3.27
5	4.4	2.06	3.29
6	4.38	2.04	3.29
7	4.38	2.07	3.31
8	4.39	2.08	3.32
9	4.4	2.13	3.32
10	4.38	1.95	3.13
11	4.38	2.04	3.29
12	4.4	2.09	3.34
13	4.36	2.09	3.35
14	4.4	2.02	3.32
15	4.41	2.03	3.17
16	4.41	2.09	3.31
17	4.38	2.02	3.33
18	4.41	2.13	3.34
19	4.37	2.04	3.32
20	4.35	2.06	3.29
21	4.4	2.01	3.31
22	4.36	2.12	3.38
23	4.39	2.04	3.28
24	4.41	2.06	3.23

Table S16 Band gaps (eV) of the X-CTO system estimated by hybrid-DFT calculation (HSE06).

Replaced site	X = Li	X = Na	X = Ag
1	1.64	1.64	1.65
2	1.65	1.65	1.65
3	1.65	1.65	1.65
4	1.64	1.66	1.66
5	1.64	1.65	1.65
6	1.64	1.65	1.64
7	1.64	1.65	1.64
8	1.64	1.65	1.64
9	1.64	1.64	1.63
10	1.63	1.63	1.65
11	1.64	1.64	1.64
12	1.64	1.64	1.64
13	1.65	1.65	1.64
14	1.65	1.65	1.65
15	1.62	1.64	1.64
16	1.63	1.63	1.64
17	1.66	1.66	1.65
18	1.64	1.64	1.64
19	1.64	1.65	1.65
20	1.64	1.65	1.65
21	1.65	1.66	1.65
22	1.65	1.66	1.64
23	1.65	1.65	1.64
24	1.64	1.64	1.64

Table S17 Band gaps (eV) of the X-ATO system estimated by hybrid-DFT calculation (HSE06).

Replaced site	X = Li	X = Na	X = Cu
1	2.87	2.88	1.99
2	2.86	2.86	2.03
3	2.89	2.87	2.03
4	2.87	2.89	2.2
5	2.85	2.85	2.08
6	2.85	2.87	1.99
7	2.84	2.88	2.03
8	2.85	2.87	1.99
9	2.87	2.88	2.08
10	2.91	2.90	2.00
11	2.86	2.87	2.05
12	2.88	2.90	2.15
13	2.87	2.92	2.08
14	2.91	2.86	2.05
15	2.92	2.89	1.97
16	2.91	2.85	2.09
17	2.89	2.90	2.02
18	2.83	2.86	2.08
19	2.84	2.90	2.04
20	2.81	2.87	1.96
21	2.82	2.84	2.00
22	2.86	2.87	2.15
23	2.85	2.86	1.99
24	2.92	2.90	2.06

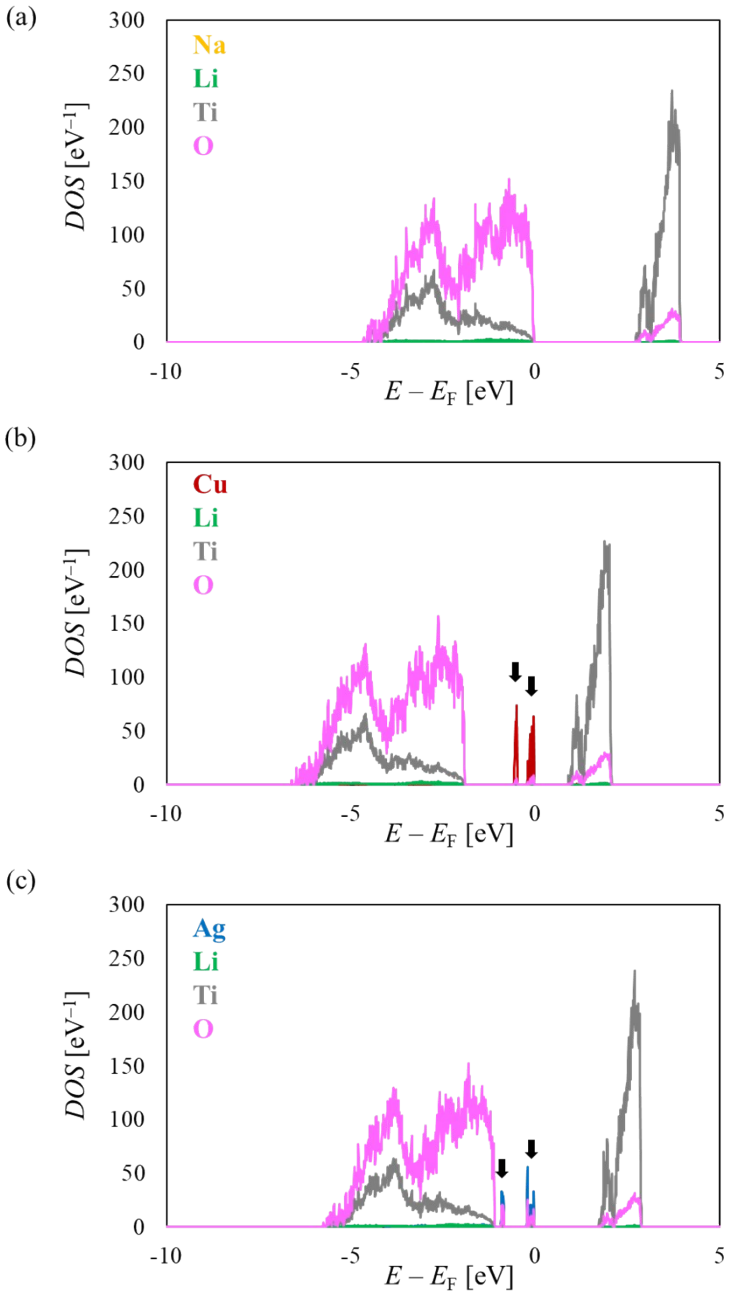

Fig. S10. Projected density of states (PDOS) of the most stable of the Na-LTO (a), the Cu-LTO (b), and the Ag-LTO (c). Arrows indicate the new peaks created by partial substitutions.

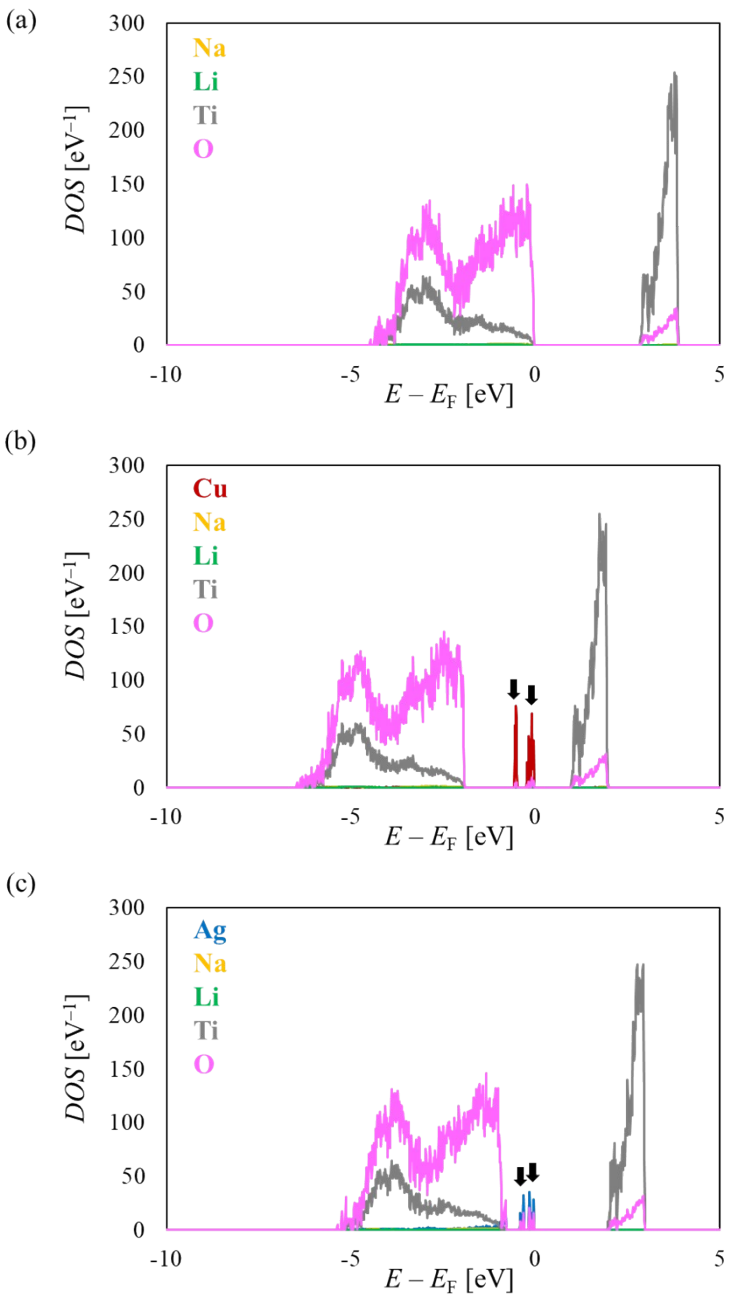

Fig. S11. Projected density of states (PDOS) of the most stable of the Li-NTO (a), the Cu-NTO (b), and the Ag-NTO (c). Arrows indicate the new peaks created by partial substitutions.

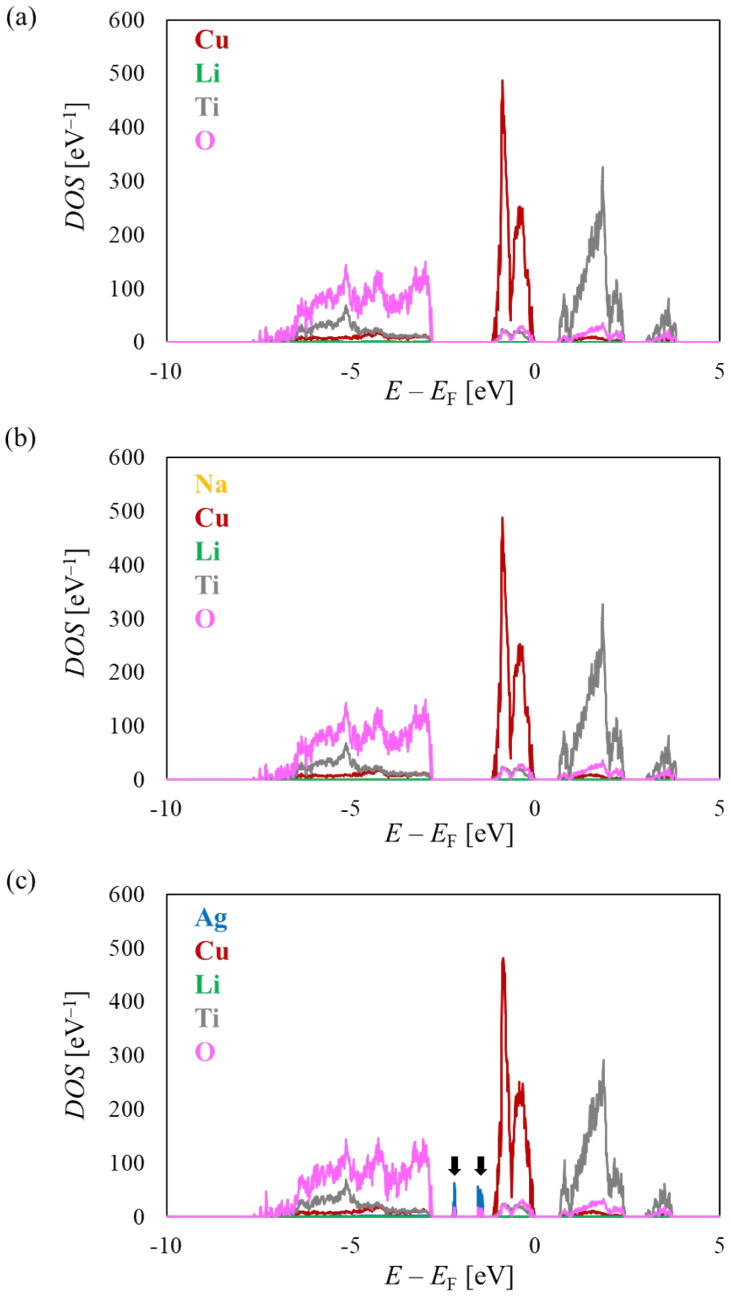

Fig. S12. Projected density of states (PDOS) of the most stable of the Li-CTO (a), the Na-CTO (b), and the Ag-CTO (c). Arrows indicate the new peaks created by partial substitutions.

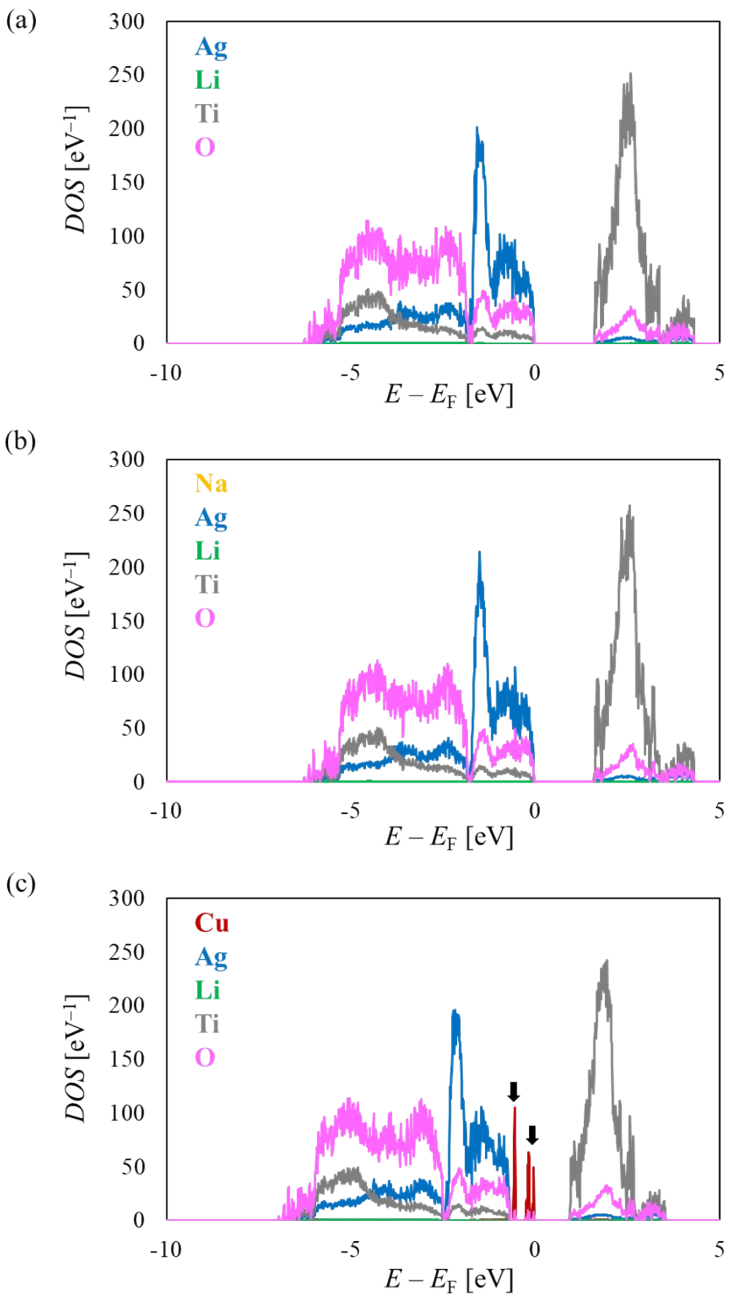

Fig. S13. Projected density of states (PDOS) of the most stable of the Li-ATO (a), the Na-ATO (b), and the Cu-ATO (c). Arrows indicate the new peaks created by partial substitutions.

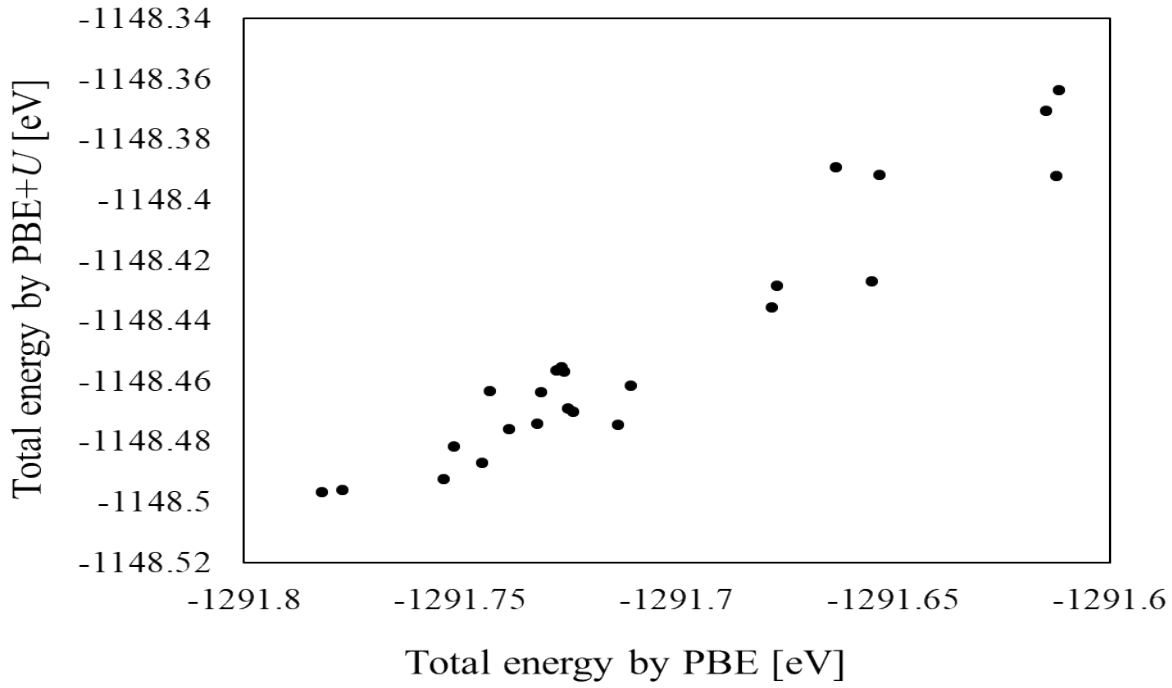

Fig. S14. Relationship between total energies of Ag-NTO estimated by PBE and PBE+*U* (*U* = 5 eV).